

# NARX-GA-Elman Method for Mach Number Prediction of Wind Tunnel Flow Field

SHAO Yawen, ZHAO Luping\*

(College of Information Science and Engineering, Northeastern University, Shenyang 110819, China.)

**Abstract:** Mach number is a key metric in the evaluation of wind tunnel flow field performance. This complex process of wind tunnel test mainly has the problems of nonlinearity and time lag. In order to overcome the problems and control the Mach number stability, this paper proposes a new method of Mach number prediction based on a nonlinear autoregressive exogenous-genetic algorithm-Elman (NARX-GA-Elman) model, which adopts NARX as the basic framework, determines the order of the input variables by using the false nearest neighbor (FNN), and uses the dynamic nonlinear network Elman to fit the model, and finally uses the global optimization algorithm GA to optimize the weight thresholds in the model to establish the Mach number prediction model with optimal performance under single working condition. By comparing with the traditional algorithm, the prediction accuracy of the model is improved by 61.5%, and the control accuracy is improved by 55.7%, which demonstrates that the model has very high prediction accuracy and good stability performance.

**Keywords:** Wind Tunnel System, Predictive Control, Mach Number Prediction, NARX-GA-Elman

## 1 Introduction

Wind tunnel tests play a vital role in the development of the aerospace field. By simulating real flight environments, wind tunnel tests can provide valuable data and information to provide a scientific basis for the design, improvement and optimization of aircraft. Wind tunnel tests can accurately measure the aerodynamic performance of a vehicle under different speeds and airflow conditions, such as lift, drag and lateral forces. These data are essential for determining the flight characteristics and performance of the vehicle. By testing different design parameters in a wind tunnel, engineers can evaluate the effectiveness of different design options and make adjustments and improvements based on the results. Wind tunnel testing also provides an in-depth study of the aerodynamic stability and control characteristics of the aircraft to

ensure the safety and maneuverability of the aircraft. All aspects of aircraft performance have been well analyzed through wind tunnel tests, and the structure of various parts of the aircraft has been improved<sup>[1]</sup>.

Improving the Mach number control accuracy as well as stability is the difficulty of wind tunnel systems<sup>[2]</sup>. With the increase of wind tunnel Mach number control requirements, the traditional PID algorithm can no longer meet the accuracy requirements. The intricate nature and stringent demands of wind tunnel systems pose challenges to the precise control of Mach numbers. However, these problems can be solved by advanced control algorithms such as predictive control. Predictive control was introduced by Richard Bellman, an American control engineer, in the 1950s<sup>[3]</sup>. He introduced the idea of dynamic programming in his study of optimal control of dynamic systems and

applied it to the field of control. The approach leverages the dynamic variations of the controlled system and optimization techniques to derive a control strategy that effectively addresses time delays and mitigates inter-variable dependencies. In predictive control systems, the predictive model assumes a crucial role by utilizing historical data to forecast the future output of the controlled object. By leveraging this prediction, the control system can proactively optimize control actions in advance, resulting in enhanced precision and accuracy. An example is a predictive control-based autonomous driving system proposed in 2019 for safe and efficient driving in urban environments. The system uses sensors to obtain real-time environmental information, predicts future traffic conditions by building a predictive model, and adjusts the vehicle's control strategy in real time based on the prediction results. The experimental results show that the predictive control system can effectively predict and adapt to complex urban traffic situations to improve driving safety and efficiency<sup>[4]</sup>.

There are two main predictive modeling methods for wind tunnel research, which are divided into mechanistic modeling<sup>[5]</sup> and data-driven modeling<sup>[6]</sup>. Mechanistic modeling is a method to study and optimize wind tunnel experiments by analyzing the structure and operational characteristics of the wind tunnel circulation in order to build an aerodynamic model. For example, in 1991, Soeterboek R.A.M. et al. used the Throwpan diagram equation and performed several estimations in order to predict Mach number. Nevertheless, the process modeling and prediction methods employed were too rudimentary to achieve satisfactory control performance.<sup>[7]</sup> The more prevalent data-driven modeling techniques nowadays utilize field data to establish the mapping relationships between the system's parameters and inputs/outputs. For example, Xu addressed the nonlinear characteristics and time lag in rail transit passenger flow by employing various predictive models. The results indicated that the Nonlinear Autoregressive Network Exogenous Inputs (NARX) model outperformed the others in terms of accuracy in predicting passenger flow<sup>[8]</sup>. Similarly NARX is

widely used in the wind tunnel field. In 2013, Dandois J. used NARX model with external inputs to identify the pressure signals in the wind tunnel system<sup>[9]</sup>.

Wind tunnel modeling mechanism modeling is very difficult, and there are more scholars studying data modeling at present, however, due to the wind tunnel system has the characteristics of frequent perturbation, nonlinearity, time lag, and many working conditions, which leads to that the Mach number control accuracy of the existing research methods can not be limited to 0.001<sup>[10]</sup>. Therefore, a new Mach number modeling method NARX-GA-Elman is proposed in this paper. This approach utilizes the NARX model architecture as the fundamental framework, which effectively addresses the challenge of dynamic time lag. Solve for the order using the FNN algorithm. This method fits the model with the dynamic nonlinear network Elman, introduces the GA algorithm for the optimization of weights and thresholds, and finally compares this algorithm with the traditional algorithm to show the outstanding capabilities of the predictive model.

## 2 NARX-GA-Elman Method

### 2.1 NARX Basic Framework

The NARX model is commonly used for modeling time series, which not only can be over-advanced prediction, but also well overcomes the problem of error accumulation caused by using the prediction model for multi-step prediction in predictive control.

In this paper, the NARX model is used as the basic framework to solve the time lag problem in wind tunnels, which was originally proposed by Billings et al. in 1985<sup>[11,12]</sup>. This model offers several advantages over alternative models, including a reduced number of identification parameters, superior approximation accuracy, and enhanced generalizability. The NARX model requires historical input and output data to determine the predicted output using a nonlinear function. The fundamental equation of the model at time  $t$  can be represented as:

$$\tilde{y}(t) = f(y(t-1), \dots, y(t-n_y), x(t-1), \dots, x(t-n_x)) \quad (1)$$

Where  $y(t-1), \dots, y(t-n_y)$  and  $x(t-1), \dots, x(t-n_x)$  denote the historical output, input sequence of the system, respectively;  $\tilde{y}(t)$  denotes the predicted output;  $n_x, n_y$  denotes the input and output variable orders, respectively;  $f$  denotes the nonlinear function. Fig.1 depicts the architecture of the NARX model.

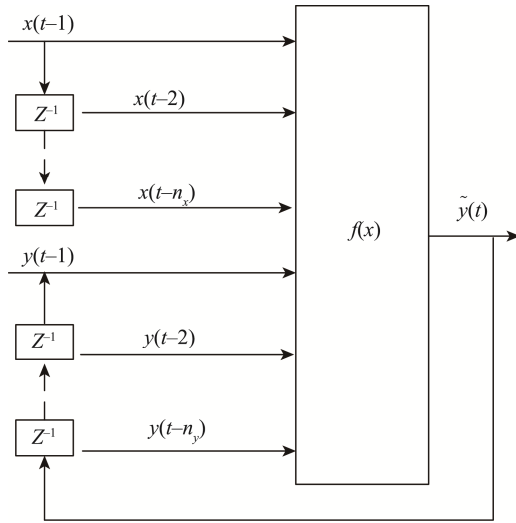


**Fig.1 Architecture of the NARX Model**

In NARX modeling, the crucial aspect lies in determining the variable order within the model and selecting an appropriate nonlinear fitting function. If the variable order is chosen improperly, it may result in challenges related to algorithm storage. Additionally, the accuracy of the model can be influenced by the fitting method employed. The selection of variable orders in NARX modeling commonly involves methods such as the Correlation Integral (CI) method<sup>[13]</sup>, Singular Value Decomposition (SVD) method<sup>[14]</sup>, and False Nearest Neighbor (FNN) method<sup>[15]</sup>. These methods assist in determining the appropriate order of variables within the NARX model. The CI method necessitates a substantial amount of data samples in order to be effective and has the effect of noise, which makes it difficult to compute. The singular value decomposition method is more appropriate for linear systems and may not be as suitable for nonlinear systems. Also the decomposition

can only be done for square arrays, however most of the practical systems that need to be decomposed are not square arrays.

Hence, this paper employs the FNN method, which is grounded in the concept of space unfolding, for selecting the variable order. As the spatial dimension rises, it makes the neighboring points squeezed together separate. The optimal variable order is determined by the FNN method based on the criterion of the neighboring points disappearing until the minimum spatial dimension is reached. Fig.2 illustrates the schematic diagram of the FNN method. For points A, B, and C in the same orbit in one-dimensional space, since the orbits are not sufficiently separated, points A, B, and C are neighboring points; when the spatial dimensionality is raised to two dimensions, C is still a neighboring point for point B, and point A, which is far away from B and C due to the elevated dimensionality, is a pseudo-neighboring point for B.

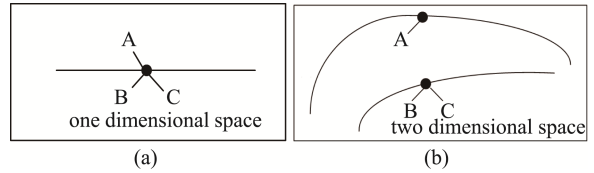


**Fig.2 Diagram of False Nearest Neighbor**

The FNN algorithm can be described by the following formula:

In the case of available sample data:

$$x_k = [y(k-1), \dots, y(k-n), u(k-1), \dots, u(k-n)]^T \quad (2)$$

In the FNN algorithm, we search for the nearest neighbor point  $x_j^n$  in an  $n$  dimensional space that minimizes the distance to a target point  $d_n$ .

$$d_n = \|x_k^n - x_j^n\|_2 \quad (3)$$

Determine whether the following description is true or false:

$$\frac{|y_k - y_j|}{\|x_k^n - x_j^n\|_2} \leq R \quad (4)$$

The FNN algorithm employs a critical value  $R$ , typically set between 10 and 50 (usually taken as 10), to determine the validity of the formula mentioned above. If the formula is found to be false, it indicates

that the point under consideration is a pseudo-nearest neighbor point.

## 2.2 Elman Neural Network

In model determination, not only does the order of the variables have an important effect on the model, but the selection of an appropriate nonlinear fitting function is also extremely important. To capture the nonlinear mapping relationship between the inputs and outputs, a nonlinear fitting function is chosen. This function is carefully selected to exhibit strong nonlinearity and ensure good generalization performance.

The Elman neural network, developed by J.L. Elman in 1990<sup>[16]</sup>, is a recurrent neural network that incorporates state feedback and has high computational power, making it a typical example of such networks. The Elman neural network introduces a context layer based on the hidden layer of the BP model, which acts as a delay operator and incorporates a memory function. This allows the network to effectively handle dynamic and time-varying characteristics, while also ensuring global stability. The Elman-type neural network typically consists of four layers: input layer, hidden layer, context layer, and output layer. The specific architecture is shown in Fig.3.

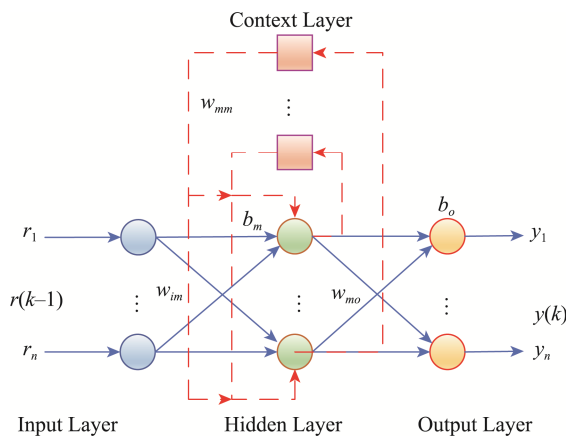


**Fig.3 Diagram of Elman Network Structure**

The Elman-type neural network is structured similarly to a feed-forward network, with input, hidden, and output layers. In this network, the input layer

serves as a means of signal transmission, while the output layer performs linear weighting functions. The transfer function of the units in the hidden layer can be either linear or nonlinear. The context layer, also known as the undertaking layer or state layer, is responsible for storing the previous output value of the hidden layer units and reintroducing it as a one-step delayed operator into the network's input. By capturing and learning from the intermediate states, the network gains nonlinear mapping capabilities and robust dynamic memory, making it an effective model for describing the dynamics of the original system.

In this paper, the input vector at moment  $k$  of the prediction model is denoted as  $r(k)$

$$r(k) = (x_1(k-1), \dots, x_1(k-n_1), \dots, x_n(k-1), \dots, x_n(k-n_n), y_1(k-1), \dots, y_1(k-n_{o1}), \dots, y_q(k-1), \dots, y_q(k-n_{oq})) \quad (5)$$

The Elman neural network is employed as a nonlinear function for fitting in the model. The number of input layers is denoted as  $r = n_1 + \dots + n_n + n_{o1} + \dots + n_{oq}$ , the number of output layers is denoted as  $q$ , and the number of intermediate and successor layers is denoted as  $l$ . Typically, the determination of the number of hidden layers is made based on the following equation:

$$l = \sqrt{r + q} + a \quad (6)$$

where  $a$  is a constant between 1 and 10, usually set around 5<sup>[17]</sup>.

At moment  $k$ , when the input  $r(k)$ , after the neural network, the predicted output is  $Y(k)$ .

$$Y(k) = f_o(W_{mo}x(k) - B_o) \quad (7)$$

$$x(k) = f_m(W_{mm}x_C(k) + W_{im}r(k-1) - B_m) \quad (8)$$

$$x_C(k) = x(k-1) \quad (9)$$

$$W_{im}(l \times n) = \begin{bmatrix} w_{i1} & \dots & w_{in} \\ \vdots & \ddots & \vdots \\ w_{il} & \dots & w_{ln} \end{bmatrix} \quad (10)$$

$$B_m(l \times 1) = [b_1 \dots b_l]^T \quad (11)$$

$$W_{mm}(l \times l) = \begin{bmatrix} w'_{11} & \dots & w'_{1l} \\ \vdots & \ddots & \vdots \\ w'_{l1} & \dots & w'_{ll} \end{bmatrix} \quad (12)$$

$$W_{mo}(q \times l) = \begin{bmatrix} w''_{11} & \dots & w''_{1l} \\ \vdots & \ddots & \vdots \\ w''_{q1} & \dots & w''_{ql} \end{bmatrix} \quad (13)$$

$$B_o(q \times 1) = [b_1 \dots b_q]^T \quad (14)$$



where at moment  $k$ ,  $\mathbf{x}(k)$  is an  $l$  dimensional intermediate layer node vector; The vector  $\mathbf{x}_c(k)$  represents a feedback state with a dimensionality of  $l$ ; The matrix  $\mathbf{W}_{im}$  represents the weight connections between the input layer and the intermediate layer; The matrix  $\mathbf{B}_m$  denotes the threshold values for each neuron in the intermediate layer; The matrix  $\mathbf{W}_{mo}$  represents the weight connections between the intermediate layer and the takeover layer; The mapping function from the input layer to the intermediate layer is denoted by the matrix  $f_m$ , and the selected function for this mapping is the Sigmoid (S-type) function. is the mapping function selected by the input layer to the intermediate layer, and the S-type function is used in this paper; The matrix  $\mathbf{W}_{mo}$  captures the weight connections between the intermediate layer and the output layer; The matrix  $\mathbf{B}_o$  represents the threshold values for each neuron in the output layer; In this paper, the mapping function from the intermediate layer to the output layer is denoted by the matrix  $f_o$ , and a linear function is chosen for this mapping.

To evaluate the model's performance, the global error  $E$  is computed using  $K$  samples of training data.:

$$E = \frac{1}{2K} \sum_{k=1}^K (Y(k) - \tilde{Y}(k))^2 \quad (15)$$

where  $Y(k)$  is the actual output at the current moment;  $\tilde{Y}(k)$  is the model predicted output.

### 2.3 Genetic Algorithm

Elman neural networks are recognized for their exceptional dynamic properties and robust global stability, making them a popular choice for handling complex, nonlinear, and dynamic data. However, despite being an optimized version of the back-propagation (BP) neural network, the Elman model still inherits certain inherent limitations that can impact its accuracy and performance. To overcome these shortcomings, the Genetic Algorithm (GA) is introduced into the Elman algorithm to optimize the connection weights and thresholds. This integration effectively prevents the neural network from getting trapped in local minima during training, leading to significant improvements in both training speed and

accuracy.

Genetic algorithms, also known as evolutionary algorithms, modeled on the idea of the theory of biological evolution proposed by Darwin. It is to randomly select individuals in a limited range, keep the individuals with strong adaptive ability according to the individual fitness, eliminate the bad individuals, and update and replace them until the optimal result is approached.

In 2018, Hamizah R. et al. estimated the model parameters in the model of the effect of ionizing radiation on target cells by using pattern search and genetic algorithm, respectively, and showed that the genetic algorithm was more superior by comparing the computation time and prediction error<sup>[18]</sup>. In 2021, Xu X. et al. chose the Elman neural network as a fast and effective identification of the source of the sudden water as the basis of the discriminative model, optimized elman neural network (ENN) by the genetic algorithm, and created an improved discriminative model called GA-ENN. The selection of representative and accurate hydration data effectively improved the effectiveness of the identification of sudden water sources in mines<sup>[19]</sup>. In 2022, Song H.Y. et al. used genetic algorithms to optimize the operating parameters of the refrigeration system of an electric refrigerated truck, and successfully reduced the energy consumption of the refrigerated truck<sup>[20]</sup>.

The implementation process of a genetic algorithm consists of the following steps:

Step 1: Initialize the population

The initial population, which represents the number of individuals contained in the population, generally takes a value in the range of 20-100.

Step 2: Coding and decoding

The encoding method largely determines how to carry out the genetic evolution operation of the population and the efficiency of genetic evolution. The main coding methods are binary coding, floating point coding, symbolic coding, multi-parameter coding, variable length chromosome coding and so on. The binary coding method is widely used because of its simple and logical operation. Binary coding

consists of a binary symbol set of binary symbols 0 and 1.

If a set of parameters takes values in the range  $[U_1, U_2]$ , and the values in that range are represented by a binary encoding, a set of  $2^k$  different encoding is produced:

$$\begin{aligned} 0000 \cdots 0000 &= 0 \rightarrow U_1 \\ 0000 \cdots 0001 &= 1 \rightarrow U_1 + \delta \\ 0000 \cdots 0010 &= 2 \rightarrow U_1 + 2\delta \\ &\vdots \\ 1111 \cdots 1111 &= 2^k - 1 \rightarrow U_2 \end{aligned} \quad (16)$$

where  $\delta = \frac{U_2 - U_1}{2^k - 1}$ .

Since the data is encoded, when the solving process is completed, the corresponding decoding operation is performed on the data. Assuming that the binary encoding of a particular body is  $b_k b_{k-1} \cdots b_2 b_1$ , the data after decoding is:

$$X = U_1 + \left( \sum_{i=1}^k b_i 2^{i-1} \right) \times \frac{U_2 - U_1}{U_2} \quad (17)$$

#### Step 3: Selection

The role of the selection algorithm in genetic algorithms is to select the best individuals from the previous generation of the population to be inherited into the next generation of the population. Usually, a roulette wheel selection method is used to assign individuals the probability of being selected according to their fitness values. In a population with  $M$  individuals, where the fitness value of the  $i$ -th individual is denoted as  $F_i$ , we can determine the probability,  $P_i$  of selecting the  $i$ -th individual as follows:

$$P_i = \frac{F_i}{\sum_{n=1}^M F_n} \quad (18)$$

#### Step 4: Crossover

The crossover operator is used to generate offspring, which is achieved by swapping the genes at a certain defined crossover position of the two parents. The crossover operation is performed with a certain probability, which is called the crossover rate and is usually set between 0.5 and 0.95.

#### Step 5: Mutation

The basic element of the variation operator is to make changes to the gene values at certain gene positions of an individual. Using the basic position mutation algorithm, the operation steps for basic position mutation include: first determine the gene mutation position of each individual coding string, then set a probability of mutation, and finally take the original gene of the inverse mutation point according to the probability. This probability is very small, generally in the range of 0.01 to 0.1.

#### Step 6: Calculation of fitness

Used to evaluate the fitness of a certain chromosome, the fitness function is usually selected by transforming the objective function into a fitness function that seeks to maximize its value. If the objective function  $f(x)$  is known, then

(1) If  $f(x)$  is a maximum optimization problem, then the fitness function:

$$Fit(f(x)) = f(x) \quad (19)$$

(2) If  $f(x)$  is a minimax optimization problem, then the fitness function:

$$Fit(f(x)) = \frac{1}{f(x)} \quad (20)$$

The iterative process of the algorithm reaches convergence, leading to the termination of the algorithm when the given number of evolutionary generations is satisfied or the termination condition for the algorithm is met when either the fitness of the optimal individual reaches a predefined threshold or the fitness of both the optimal individual and the population no longer increase. Otherwise, the previous generation of population is replaced with the new generation of population obtained through selection, crossover and mutation, and returns to step 3. Fig.4 illustrates the flowchart of the algorithm.

## 2.4 NARX-GA-Elman Model

Combining the methods mentioned in 2.1, 2.2 & 2.3 above, in order to solve the problems such as time lag in the wind tunnel system, so that the Mach number accuracy is more accurate and meets the requirements of the project, this paper establishes the NARX-

GA-Elman model, with NARX as the basic framework, FNN for order determination, and fitting through elman dynamic nonlinear network, using Elman neural network algorithm optimized by genetic algorithms, to construct such a model through GA algorithm for chromosome encoding, calculation of the fitness function to retrain the model until the optimal solution is found. The corresponding model of NARX-GA-Elman is shown in Fig.5.

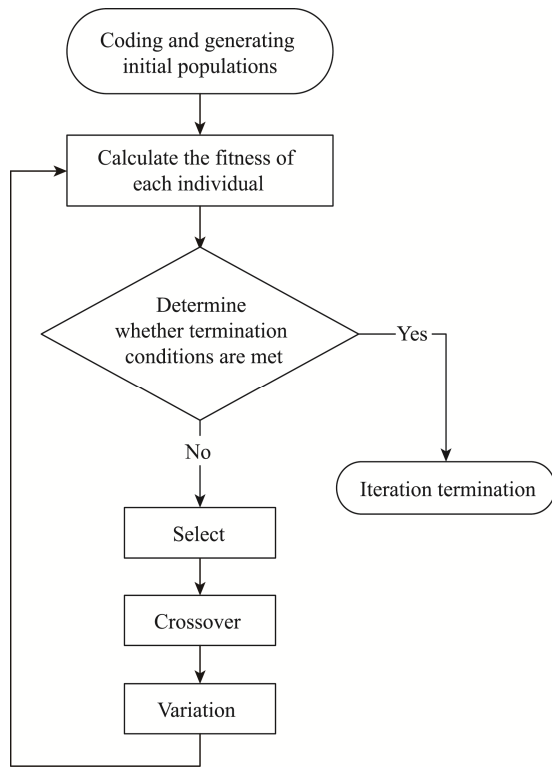


Fig.4 Flowchart of Genetic Algorithm

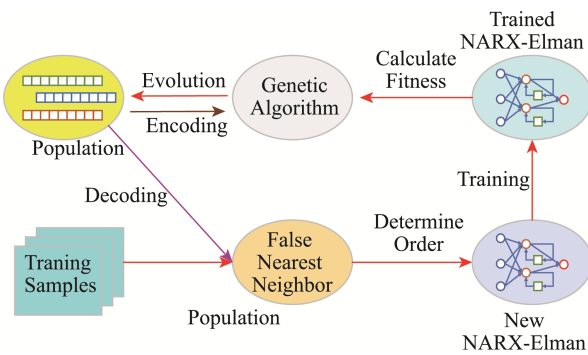


Fig.5 Flowchart of NARX-GA-Elman Algorithm

### 3 Experimental Description of Wind Tunnel System

#### 3.1 Wind Tunnel Structure and Key Parameters

The object of this paper is the 0.6-meter continuous transonic wind tunnel, FL-61 wind tunnel, which was constructed by AVIC Aerodynamic Research Institute and completed at the end of 2012, and is mainly used for the development of large aircraft. In order to improve the accuracy of Mach number prediction, it is necessary to know enough about the current wind tunnel and fully analyze it in order to build a more accurate Mach number prediction model. Fig.6 illustrates the structure of the continuous transonic wind tunnel.

The main parts of the continuous wind tunnel are the compressor, the cooling section and the test section. The compressor, as the power source of the whole system, is called the heart of the continuous wind tunnel. The compressor is driven by two DC motors in series, installed in the power section, located between the second diffusion section and the second corner, through the rotation of the compressor blades, the wind needed for the wind tunnel test is blown. The compressor is used to change the rotational speed of the compressor through the frequency converter to change the air flow speed inside the cave, thus changing the static pressure in the resident section to simulate the air condition around the tested aircraft model, through which the compressor can make the airflow flow continuously inside the wind tunnel, with the rotational speed control accuracy of  $\leq 0.1\%$ . The compressor can not only change the airflow by changing the rotational speed, but also change the blade angle to affect the airflow inside the cave, the blade angle adjustment range is  $30^{\circ}\sim 86^{\circ}$ .

Due to the continuous addition of continuous wind tunnel compressor drive power, the temperature inside the tunnel will rise, and the high temperature will have a serious impact on the use of measurement and control equipment as well as the structure of the wind tunnel. Therefore, the cooling section in the wind

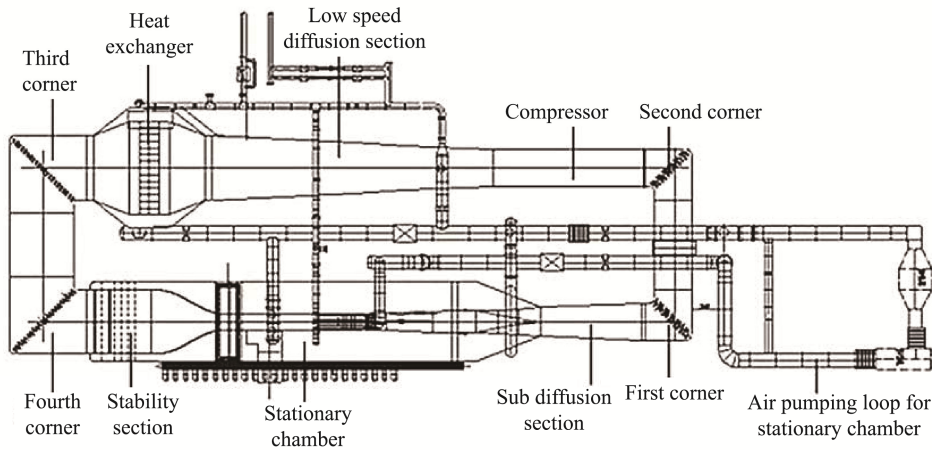


**Fig.6 Structural of the Continuous Wind Tunnel**

tunnel system to reduce the gas temperature is essential. The cooling section of this wind tunnel uses a heat exchanger to control the temperature of the gas flow. The heat exchanger, also called exchanger, is set before the third corner and mainly transfers part of the heat from the high temperature gas stream generated by the compressor to the cold fluid equipment. The heat exchanger of this wind tunnel takes the finned tube type heat exchanger with bimetallic rolled sheets.

The most important part of the wind tunnel system for observation as well as data measurement is the test section of the wind tunnel system, i.e., the place where the vehicle is tested. The test section is divided into upstream and downstream. The upstream section has a stabilization section and a contraction section. The stabilization section has a honeycomb and two sets of damping grids to improve the straightening of the airflow and reduce turbulence. The front of the stabilizing section is usually equipped with a noise-reducing sandwich for noise reduction. The contraction section is used to accelerate the gas to the desired velocity. Downstream of the test section is a sub-expansion section, which is mainly used to reduce the flow velocity. The vehicle model is mounted on a mechanism inside the chamber by means of struts, and the angle of attack of the model is changed during the test by changing the action of the drive shaft to simulate the airflow condition after the angle of the

vehicle is changed in the air. The aerodynamic forces on the aircraft vary greatly with different angles of attack, thus, the measured hydrostatic pressure also changes.

The flow field of the continuous wind tunnel is a multivariate complex system. Based on the aforementioned analysis of the aerodynamic structure, it is evident that the primary control parameter for the continuous wind tunnel is the rotational speed ( $S$ ) of the compressor, and there are two disturbing quantities, which are the stabilized section total pressure ( $P_0$ ) and the model angle of attack ( $A_n$ ). The main controlled variable in a wind tunnel system is the Mach number ( $Ma$ ), requiring Mach number control accuracy  $|\Delta Ma| \leq 0.001$ .

### 3.2 Selection of Wind Tunnel Test Conditions

This wind tunnel requires a large number of parameter settings before the variable angle of attack test. Firstly, it is necessary to set the operating Mach number for the current operating conditions, and the different set values of Mach number lead to different gas flow rates in the wind tunnel, so that the change of the model's angle of attack has a different impact on the Mach number, and the characteristics of the system are changed. The wind tunnel studied in this paper has carried out a large number of experimental blowing, during which a wealth of data has been accumulated, which is an inherent advantage for the use of data

modeling, but these data can not contain all the operating conditions at present. Working conditions are mainly determined by the demand for wind blowing, the different demand for wind blowing leads to the accumulation of data under various working conditions is not exactly the same, specifically in several working conditions run more often, the accumulated data is sufficient, and some of the working conditions are insufficient, so this paper selects three kinds of data accumulated more sufficiently as a typical working conditions, and uses this part of the data as the modeling data to establish the Mach number prediction model. The data investigated in this paper are for the transonic range with Mach numbers between 0.8 and 1.0. There are mainly two kinds of blade angles,  $76.5^\circ$  and  $56.3^\circ$ , and two kinds of change speeds of the angle of attack,  $0.1^\circ/\text{s}$  and  $0.2^\circ/\text{s}$ , and the working conditions are set as shown in Table 1.

**Table 1 Working Conditions of the Wind Tunnel Flow Field**

Conditions	Mach Number	Sample Size
1	0.8	1626
2	0.85	1057
3	0.9	752

### 3.3 Main Difficulties in Wind Tunnel Modeling

Since the dimensions and structures of different wind tunnels are different. Modeling wind tunnel systems also faces a variety of challenges, which requires researchers to continuously explore wind tunnel-specific modeling methods. In general, for modeling a single operating condition, it is necessary to first test the current operating condition, then analyze and model the data, and finally test and control the current operating condition. However, this is undoubtedly time-consuming and laborious, and also causes a great waste of resources, which puts forward new requirements for modeling.

#### (1) Difficulty in modeling mechanisms

Although mechanistic modeling has been developed earlier and is capable of describing the wind tunnel operation process as a whole, there are

non-negligible problems. On the one hand, mechanistic modeling requires a priori knowledge and a combination of theory and experience based on expert and specific knowledge. For wind tunnel systems, a good understanding of aerodynamic theory and wind tunnel operation mechanisms is required, and the laws of aerodynamics are obscure and difficult to interpret for scholars who are not specialized in this field. On the other hand, since most of the mechanism models simplify the complex three-dimensional flow of air into one-dimensional flow, it is difficult to describe the complex structure inside the wind tunnel system as well as the external perturbations, although the overall volume of the wind tunnel system can be predicted better. If higher Mach number control accuracy is required, the mechanistic model cannot be adapted to the development of wind tunnels.

#### (2) Frequent disturbances

During wind tunnel tests, changes in angle of attack can lead to large deviations in the Mach number, while continuous changes in angle of attack during continuous variable angle of attack tests can lead to continuous perturbations in the system, which makes the control and modeling process exceptionally difficult.

#### (3) Nonlinear

In wind tunnel tests, the flow field characteristics vary greatly at different Mach number conditions. For example, at Mach 0.7, a change in rotational speed of 1 revolution resulted in a change in Mach 0.00058; at Mach 0.9, a change in rotational speed of 1 revolution resulted in a change in Mach 0.00071.

#### (4) Lagging

Due to the long and wide ducts of the wind tunnel system, the compressor that generates the airflow is far away from the actual model, the airflow needs to pass through the diffusion section, the third and fourth corners and the stabilizing section before it reaches the model, and the sensors for measurements are not in the same position as the model, so it leads to time lag problems in the system.

#### (5) High prediction accuracy requirements

Currently, the project requirements for the Mach number prediction model predict the root mean square

error to be within 0.001.

(6) Multiple working conditions

The continuous wind tunnel is equipped with a variety of experimental equipment, such as elicitation slits, opening and closing ratios, blade angles, etc. Any change in the position of the equipment will produce a new working condition. Secondly, the different set values of total pressure, Mach number, and angle of attack change will also lead to the change of working conditions. Only for a wind tunnel system, there can be hundreds of working conditions, increasing the difficulty of modeling.

(7) High energy consumption

Usually, for an airplane model, there are dozens or even hundreds of tests just under different Mach numbers. Continuous wind tunnel compressor needs a motor as a driver, the motor power up to 20MW, on a test of a few dozen seconds, the cost of electricity will be nearly ten thousand dollars, the cost is very high.

### 3.4 Experimental Evaluation Indicators

For high-precision control systems of wind tunnel flow fields, the accuracy of modeling directly affects the stability of the subsequent control Mach number. In order to better assess the level of modeling, appropriate judging criteria need to be adopted to analyze the model. Usually, the Root Mean Square Error (RMSE) is chosen to judge the Mach number prediction, which quantifies the disparity between the predicted value and the actual value. The smaller the RMSE is, the greater the proximity between the predicted value and the actual value, and the more accurate the model is in predicting.

$$RMSE = \sqrt{\frac{1}{K} \sum_{k=1}^K (Ma(k) - \widetilde{Ma}(k))^2} \quad (21)$$

where  $Ma(k)$  is the actual value;  $\widetilde{Ma}(k)$  is the predicted value; and  $K$  refers to the quantity of sampling points.

For wind tunnel systems, the ultimate goal of model prediction is to perform Mach number control. In general, the Mach number is required to be stabilized around a set value, which is noted as  $Ma_{set}$ . The evaluation of the model considers the accuracy of

the prediction on the one hand, and the influence on the control effect on the other hand. In order to evaluate the control effect of the model, the Mach number accuracy (A) and maximum deviation (MD) are usually also taken for evaluation.

(1) Mach number accuracy (A) represents the difference between the desired value and the average predicted value obtained during the prediction process. A smaller Mach number accuracy indicates a higher ability of the model to accurately depict the overall fluctuation in Mach number during the test section run. The formula for calculating Mach number accuracy is provided below.

$$A = |Ma_{set} - \frac{1}{K} \sum_{k=1}^K \widetilde{Ma}(k)| \quad (22)$$

(2) Maximum deviation (MD) is the maximum prediction deviation between the actual and predicted values. As an important performance indicator, the solution of the maximum deviation yields whether the model predictions meet the requirements and whether the model is stable. The formula for the maximum deviation is as follows, and the maximum deviation of the Mach number is required to be no more than 0.001.

$$MD = \max |Ma(k) - \widetilde{Ma}(k)| \quad (23)$$

## 4 Results and Discussion

Firstly, the FNN algorithm is utilized to determine the order of each variable. Taking condition 3 as an example, Fig. 7 shows the order analysis of the input variables, respectively, and the order of variable analysis is selected from 1 to 15. Analyzing the order of the total pressure in Fig. 7(a), when the order is 4, the proportion of pseudo-nearest neighbor is 0, and the neighboring point disappears, therefore, the optimal order of the total pressure is selected to be 4. Similarly, the optimal order of the rotational speed, the angle of attack, and the Mach number is selected to be 5, 6, and 5, respectively.

FNN is performed for all three conditions to determine the order of the variables, and different variables have different orders, but the same variable varies up to a range of three orders under different conditions, as shown in Table 2.

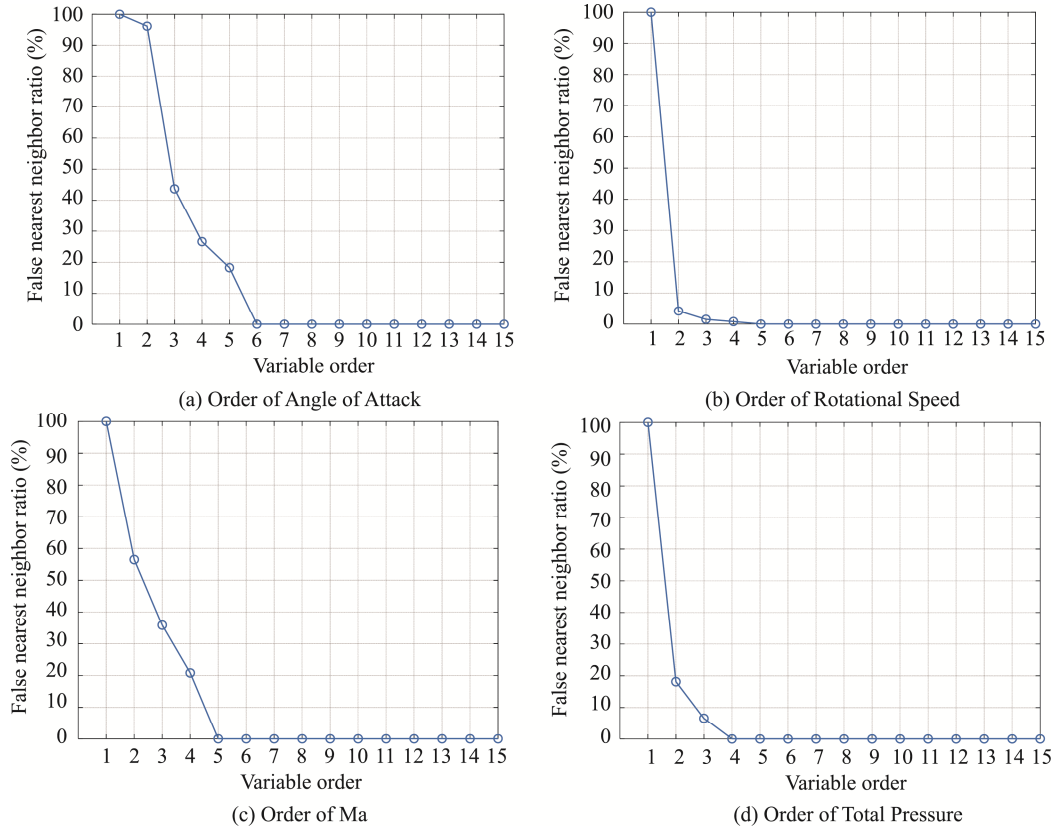


Fig.7 Order Analysis of Model Variables

Table 2 Variable Order for Different Operating Conditions

Conditions	Total Pres- sure	Rotational Speed	Angle of Attack	Mach Number
1	4	5	6	6
2	4	8	4	5
3	4	5	6	5

To enhance the selection of an appropriate order and mitigate the instability of individual test outcomes, this paper adopts multiple samples of each variable under various working conditions to analyze the variable order. The resultant optimal variable order, as demonstrated in Table 3, ensures that the test aligns closely with real-world scenarios.

Table 3 Optimal Order of Variables

Variables	Total Pres- sure	Rotational Speed	Angle of Attack	Mach Number
Best Order	4	5	6	5

In summary, the FNN algorithm is employed to establish the variable orders  $n_{p_0}$ ,  $n_s$ ,  $n_{An}$  and  $n_{Ma}$  as 4, 5, 6, and 5.

The sum of the optimal variable orders is used as the number of neurons in the input layer of the NARX-GA-Elman model, denoted as  $r = 20$ ; The model predicts only one variable, Mach number, so the output layer is denoted as  $q = 1$ ; the number of neurons in the intermediate layer is calculated according to Eq. (6), and  $\alpha$  is taken to be 5, which gives the number of intermediate neurons  $l = 10$ .

Initially, the model's weights and thresholds are randomly assigned. Through parameter adjustments and extensive experimental runs, the model is generated and further optimized. Finally, the following optimized settings parameters are selected as the best parameters for the model: the maximum number of training times is 1,000, the minimum error of the training target is 0.0001, and the learning rate is 0.005.70% of the collected data is selected as training set and 30% as validation set in each of the three



working conditions. And the NARX-GA-Elman model is used to predict the Mach number of the three working conditions, compared with the traditional

model PLS model, the Elman model, and the NARX-Elman model. Experimental Result Curves are shown in Fig.8, Fig.9 and Fig.10.

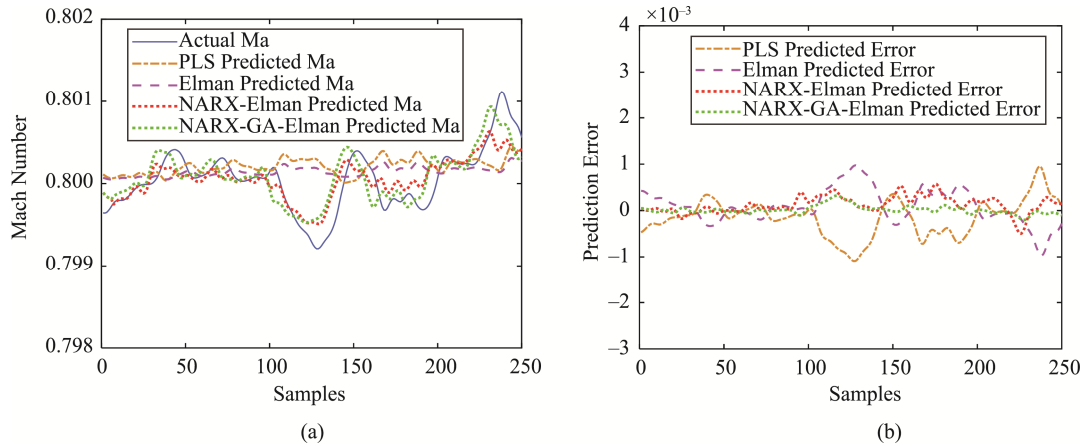


**Fig.8 (a) Prediction Curves and (b) Error Curves for Working Condition**

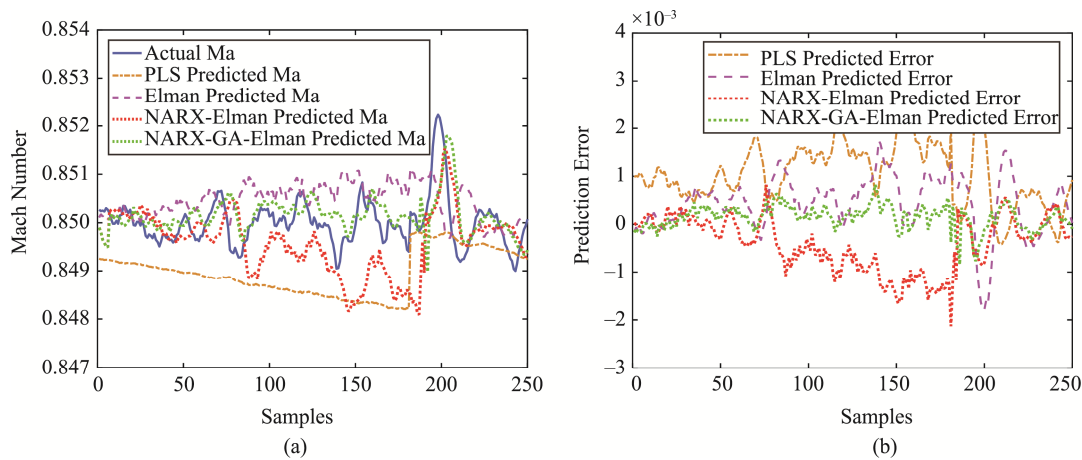


**Fig.9 (a) Prediction Curves and (b) Error Curves for Working Condition 2**

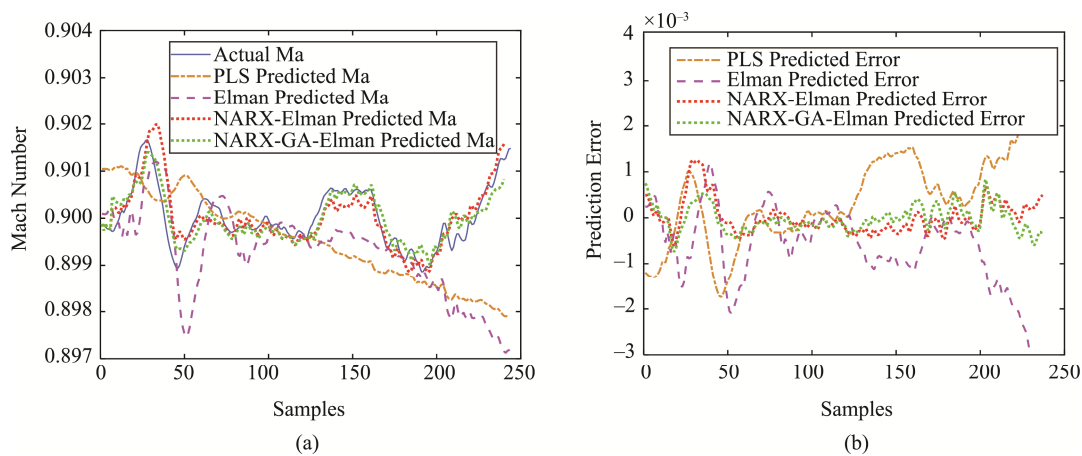


**Fig.10 (a) Prediction Curves and (b) Error Curves for Working Condition 3**



Based on the Mach number prediction plots and error plots displayed in the aforementioned three models, it can be observed that the NARX-GA-Elman model provides a more accurate prediction of the Mach

number trend. Conversely, the predictions generated by the PLS method and the Elman neural network method exhibit greater disparity from the actual Mach number trend, as indicated in Table 4.

**Table 4 Indicators for Assessing Mach Number Predictions**

Conditions	Condition I			Condition II			Condition III		
Indicators	RMSE	A	MD	RMSE	A	MD	RMSE	A	MD
PLS	0.00052	0.00034	0.00110	0.00120	0.00045	0.00360	0.00130	0.00110	0.00270
Elman	0.00044	0.00024	0.00099	0.00103	0.00074	0.00440	0.00076	0.00042	0.00230
NARX-Elman	0.00026	0.00016	0.00066	0.00036	0.00004	0.00130	0.00074	0.00044	0.00210
NARX-GA-Elman	0.00010	0.00002	0.00032	0.00028	0.00001	0.00084	0.00030	0.00014	0.00093

From the analysis in Table 4, the RMSE values of the PLS model and Elman model under working conditions 1, 2 and 3 fluctuate around 0.001, which do not meet the accuracy requirements, while the RMSE values of the NARX-Elman model and the NARX-GA-Elman model are significantly smaller than 0.001, and most of them fluctuate around 0.0003,

The A value of the three traditional models varies above and below 0.0004, while the A value of the NARX-GA-Elman model proposed in this paper is 0.00002 and 0.00001 for condition I and condition II. This indicates that the proposed model in this paper exhibits a high level of accuracy in predicting the Mach number, with minimal deviation from the preset value. Moreover, the model demonstrates consistent performance even when the situation changes, maintaining a small overall deviation.

When comparing the maximum deviation observed in the predictions made by the four models, it is evident that the majority of MD values from the remaining three models exceed 0.001 by a significant margin, while the NARX-GA-Elman model, whose MD values in the two conditions are less than 0.001, meets the project's requirements for the control accuracy, and the maximum deviation is much smaller than that of the other three models.

To sum up, the proposed NARX-GA-Elman model in this paper exhibits a significantly reduced error between the predicted value and the actual value, approaching zero. Moreover, it outperforms the PLS method, Elman method, and NARX-Elman method in terms of both the accuracy of Mach number prediction and control effectiveness. Compared with the other three models, the prediction accuracy of the NARX-GA-Elman model is improved by about

22.2%-61.5%. The control accuracy is improved by about 35.4%-55.7%, which well demonstrates the superior performance of the model.

## 5 Conclusion

Considering the nonlinearity and time lag of the wind tunnel flow field system, in order to construct a more superior model to accurately predict the Mach number, this paper proposes the NARX-GA-Elman method for Mach number prediction. The proposed approach in this paper utilizes the NARX model as the fundamental structure and uses the FNN algorithm to determine the input variable sequence and employs the dynamic Elman neural network as the nonlinear fitting function for the NARX model. GA is introduced to optimize the connection weights and thresholds of the NARX-Elman network, so that the neural network can be prevented from falling into local minima and the training speed and success rate can be improved to find the global optimal solution. The experiments compare the method proposed in this paper with three conventional models to predict the Mach number for three typical operating conditions, and the proposed method NARX-GA-Elman has better performance compared with three traditional methods. The model's Mach number prediction accuracy is improved by up to 61.5%, and the control accuracy is improved by up to 55.7%.

## Acknowledgments

This research was funded by the National Natural Science Foundation of China (No. 61503069) and the Fundamental Research Funds for the Central Universities (N150404020).

## References

- [1] Liu, Z.C. (2005). *Structural Design of Wind Tunnels*. Beijing: China Aerospace Press.
- [2] Guo, J., Zhang, R. and Cui, X. (2020). Mach number prediction and analysis of multi-mode wind tunnel system. In: *Proceedings of the 2020 Chinese Automation Congress*, Shanghai: CAC, pp.6895-6900.
- [3] Bellman, R. (1957). Dynamic Programming and Lagrange Multipliers. *Proceedings of the National Academy of Sciences*, 43(7), pp.717-719.
- [4] Smith, J., Johnson, A. and Brown, L. (2019). Predictive control for autonomous driving in urban environments. *IEEE Transactions on Intelligent Transportation Systems*, 20(5), pp.2000-2012.
- [5] Triplett, W.E. (1984). Wind tunnel correlation study of aerodynamic modeling for F/A-18 wing-store tip-missile flutter. *J. Aircr.*, 21, pp.329-334.
- [6] Brosilow, C., Tong, M. (1978). Inferential control of processes: Part II. The structure and dynamics of inferential control systems. *Aiche J.*, 1978, 24, pp.492-500.
- [7] Soeterboek, R. A. M., Pels, A. F. and Verbruggen, H. B. (1991). A predictive controller for the Mach number in a transonic wind tunnel, *IEEE Control Systems Magazine*, vol. 11, no. 1, pp.63-72.
- [8] Xu, R.J. (2017). *Research on Passenger Flow Prediction of Rail Transit Based on Time-Delay Nonlinear Autoregressive Neural Network*. Master. Chongqing University.
- [9] Dandois, J. and Pamart, P. Y. (2013). NARX modeling and extremum-seeking control of a separation. *Aerospace Lab*, 23(6), pp.1-13.
- [10] Tang, Y., Li, H. and Cai, Y. (2016). State space description based predictive control for normal temperature continuous transonic wind tunnel. In: *Proceedings of the 2016 Chinese Control and Decision Conference*, Yinchuan: CCDC, pp.28-30.
- [11] Leontaritis, I. and Billings, S. (1985). Input-output parametric models for non-linear systems part I: Deterministic non-linear systems. *Int. J. Control*, 41, pp.303-328.
- [12] Leontaritis, I. and Billings, S. (1985). Input-output parametric models for non-linear systems part II: Stochastic non-linear systems. *Int. J. Control*, 41, pp.329-344.
- [13] Broomhead, D. and King, P. (1986). Extracting qualitative dynamics from experimental data. *Phys. D Nonlinear Phenom.*, 20, pp.217-236.
- [14] Mathew, B.K. and Brown, R. (1992). Determining embedding dimension for phase-space reconstruction using a geometrical construction. *Phys. Rev. A*, 45, pp.3403-3411.
- [15] Aksamit, N. and Whitfield, P. (2019). Examining the pluvial to nival river regime spectrum using nonlinear methods: Minimum delay embedding dimension. *J. Hydrol.*, 572, pp.851-868.
- [16] Elman, J.L. (1990). Finding structure in time. *Cogn. Sci.*, 14, pp.179-211.
- [17] Han, W., Nan, L. and Su, M. (2019). Research on the Prediction Method of Centrifugal Pump Performance Based on a Double Hidden Layer BP Neural Network. *Energies*, 12, pp.2709.
- [18] Rashid, H., Siam, F.M., and Maan, N. (2018). Parameter estimation for a model of ionizing radiation effects on targeted cells using genetic algorithm and pattern search method. *Malaysian Journal of Industrial and Applied Mathematics*, pp.1-13.
- [19] Xu, X., Wang, X. and Li, K. (2021). Source discrimination of mine water inrush based on Elman neural network globally optimized by genetic algorithm. *Arabian Journal of Geosciences*, 14(13), pp.2-13.
- [20] Song, H.Y., Cai, M.H. and Cen, J. (2022). Research on energy saving optimization method of electric refrigerated truck based on genetic algorithm. *International Journal of Refrigeration*, 137, pp. 62-69.

## Author Biographies



**SHAO Yawen** is a B.Sc. candidate in Engineering from College of Information Science and Engineering, Northeastern University, China. Her main research interests include control modeling and robot vision.

E-mail: sywdream7@163.com



**ZHAO Luping** received the B.Sc. degree in automation from Northeastern University, Shenyang, China, in 2007, the M.Sc. degree in control theory from Northeastern University, Shenyang, China, in 2009, and the Ph.D. degree in control theory from the Hong Kong University of Science and Technology, Hongkong, China, in 2014. Her main research interest includes industrial process control and industrial artificial intelligence, specifically, control theory, process modeling, model migration, process monitoring, variable prediction of complex industrial processes.

E-mail: zhaolp@ise.neu.edu.cn

